



## RESEARCH ARTICLE

10.1029/2020JG005903

### Key Points:

- The “ecosystem metabolome” is presented as a concept to use the dissolved organic matter (DOM) pool as an indicator of lake ecosystem functioning and impacts thereon
- The high diversity of compounds comprising the ecosystem metabolome divides in only a few clusters based on origin and chemical properties
- Imprints of environmental drivers on the DOM pool of lakes can be elucidated by multivariate network statistics

### Supporting Information:

Supporting Information may be found in the online version of this article.

### Correspondence to:

H. P. Grossart and G. Singer,  
[hgrossart@igb-berlin.de](mailto:hgrossart@igb-berlin.de);  
[gabriel.singer@uibk.ac.at](mailto:gabriel.singer@uibk.ac.at)







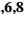
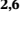

### Citation:

Fonvielle, J. A., Giling, D. P., Dittmar, T., Berger, S. A., Nejtgaard, J. C., Solheim, A. L., et al. (2021). Exploring the suitability of ecosystem metabolomes to assess imprints of brownification and nutrient enrichment on lakes. *Journal of Geophysical Research: Biogeosciences*, 126, e2020JG005903. <https://doi.org/10.1029/2020JG005903>

Received 13 JUN 2020

Accepted 8 APR 2021

## Exploring the Suitability of Ecosystem Metabolomes to Assess Imprints of Brownification and Nutrient Enrichment on Lakes

Jeremy A. Fonvielle<sup>1,2</sup> , Darren P. Giling<sup>1,3,4</sup> , Thorsten Dittmar<sup>5</sup> , Stella A. Berger<sup>1,6</sup> , Jens C. Nejtgaard<sup>1,6</sup> , Anne Lyche Solheim<sup>7</sup> , Mark O. Gessner<sup>1,6,8</sup> , Hans-Peter Grossart<sup>1,2,6</sup> , and Gabriel Singer<sup>9,10</sup> 

<sup>1</sup>Department of Experimental Limnology, Leibniz-Institute of Freshwater Ecology and Inland Fisheries (IGB), Stechlin, Germany, <sup>2</sup>Institute for Biochemistry and Biology, Potsdam University, Potsdam, Germany, <sup>3</sup>Centre for Applied Water Science, Institute for Applied Ecology, University of Canberra, Canberra, Australia, <sup>4</sup>CSIRO Land and Water, Commonwealth Scientific and Industrial Research Organisation, Canberra, ACT, Australia, <sup>5</sup>Institute for Chemistry and Biology of the Marine Environment (ICBM) and Helmholtz Institute for Functional Marine Biodiversity (HIFMB), University of Oldenburg, Oldenburg, Germany, <sup>6</sup>Berlin-Brandenburg Institute of Advanced Biodiversity Research (BBIB), Berlin, Germany, <sup>7</sup>Norwegian Institute for Water Research (NIVA), Oslo, Norway, <sup>8</sup>Department of Ecology, Berlin Institute of Technology (TU Berlin), Berlin, Germany, <sup>9</sup>Department of Ecohydrology, Leibniz-Institute of Freshwater Ecology and Inland Fisheries (IGB), Berlin, Germany, <sup>10</sup>Department of Ecology, University of Innsbruck, Innsbruck, Austria

**Abstract** Loadings of colored dissolved organic matter (cDOM) and nutrients affect lake ecosystem functioning in opposite ways, rendering assessments of combined effects challenging. We used the “ecosystem metabolome” as a conceptual framework to overcome this problem by characterizing the chemically diverse pool of DOM in lakes. The underlying rationale is that the diversity of dissolved metabolites bears the legacy of allochthonous inputs, autochthonous primary production, and a wealth of organic matter transformations resulting from microbial or photodegradation. Our objective was to assess whether high-resolution mass-spectrometric analyses can unlock that information on DOM origin and transformation pathways as well as environmental drivers imprinting the lake ecosystem metabolome. We performed a large-scale enclosure experiment to assess the influences of brownification and nutrient enrichment on the composition and diversity of DOM, and a complementary bottle incubation to isolate the effect of photodegradation. For validation, we assessed whether the same patterns emerge from published observational data from 109 Swedish lakes. Ultra-high-resolution mass spectrometry distinguished ~3000 metabolites in solid-phase extracts of lake water. Network analysis revealed five metabolite clusters that could be related to different source processes based on molecular weight, position in van Krevelen diagrams and assignment to molecular categories (peptides, lipids, etc.). Emergent DOM properties such as molecular diversity provided insights into the processes generating each of the five DOM clusters. Overall, our data suggest that the thousands of molecular formulas comprising ecosystem metabolomes of lakes arise from few major processes and reflect imprints of environmental drivers such as brownification and nutrient enrichment.

**Plain Language Summary** The brownification and eutrophication of lakes are common phenomena driven by colored dissolved organic matter (cDOM) and nutrient loading. These stressors can act simultaneously to affect the pool of DOM, a central entity in lake ecosystems consisting of thousands of organic compounds. We reasoned that the high chemical diversity of DOM can inform about the origins of the compounds, the transformation processes generating them, and the environmental context. We explored this idea by adding nutrients and colored organic compounds to a large experimental facility deployed in a lake. To assess the importance of cDOM photodegradation, we conducted a complementary bottle experiment. A high-resolution analytical technique identified almost 3,000 distinct compounds grouping into only five clusters. We assigned each cluster to a specific origin based on molecular formulas, and assessed the major processes leading to a particular group of compounds. Application of the approach to a published data set on the chemical composition of DOM from 109 lakes in Sweden indicated that our classification was transferable to natural lake ecosystems. Taken together, our results indicate that the

© 2021. The Authors.

This is an open access article under the terms of the [Creative Commons Attribution License](https://creativecommons.org/licenses/by/4.0/), which permits use, distribution and reproduction in any medium, provided the original work is properly cited.

diverse pool of dissolved organic compounds in lakes provides valuable information to pinpoint important processes as well as to identify the influence of environmental stressors.

## 1. Introduction

Freshwater ecosystems are facing a multitude of anthropogenic pressures (Hering et al., 2015), raising concerns about the future of freshwater resources and their ecological integrity (IPCC, 2014). Prominent among the many stressor-related processes affecting freshwater ecosystems are brownification and nutrient enrichment (Leech et al., 2018; Strock et al., 2017). Both of these processes directly or indirectly affect the quantity and quality of the dissolved organic matter (DOM) pool, which interacts with a range of ecosystem components and is linked to multiple ecosystem functions (Evans et al., 2005; Smith et al., 1999). Consequences range from microbial transformations of mineral nutrients and DOM at the base of the food chain to repercussions on higher trophic levels up to fish (Finstad et al., 2014; Roulet & Moore, 2006).

The widespread brownification of freshwaters, especially in northern latitudes, results in part from elevated concentrations of colored DOM (cDOM) derived from terrestrial sources (Kritzberg et al., 2020). Part of this cDOM in lakes is photodegraded or used by heterotrophic microbes, but another large fraction can persist for extended periods, affecting many aspects of ecosystem structure and functioning (e.g., Creed et al., 2015; Kritzberg et al., 2020; Solomon et al., 2015). cDOM can favor heterotrophic microbes in two distinct ways, first by providing organic resources and second by limiting primary production through strong light absorbance and hence reduced competition for nutrients with phytoplankton. As a consequence, lake ecosystems affected by brownification can shift from net autotrophy to heterotrophy (Kritzberg et al., 2020; Von Einem & Granéli, 2010).

Nutrient supply limits algal growth in many freshwaters (e.g., Lewis & Wurtsbaugh, 2008), resulting in a strong stimulation of primary production (eutrophication) when nutrient constraints are alleviated by external nutrient loading, especially of phosphorus (P) (Schindler et al., 2016; Smith et al., 1999). One of the many consequences of stimulated primary production is the release of DOM as a result of algal carbon exudation (Larsson & Hagström, 1982), viral lysis of plankton, and ‘sloppy feeding’ by herbivores benefiting from enhanced food availability (Haaber & Middelboe, 2009). In contrast to cDOM, autochthonous DOM (DOM<sub>auto</sub>) derived from algae is only weakly colored (Köhler et al., 2013) and highly bioavailable. Therefore, algal blooms induced by increased nutrient supply are followed by blooms of heterotrophic organisms, including bacterioplankton benefiting from the large quantities of organic matter of algal origin (Noble & Fuhrman, 1999; Velthuis et al., 2017). In addition, DOM<sub>auto</sub> encompasses organic matter produced and leached from aquatic organisms other than phytoplankton, including lysates and exudates from bacteria and metazoans, the growth of which was originally supported by allochthonous organic matter from terrestrial sources, at least in part.

The numerous sources fueling the DOM pool in freshwaters result in an enormous chemical diversity. Several thousand organic molecules have been identified in single lake water samples (e.g., Kellerman et al., 2014). This suggests that understanding the role of DOM in lake ecosystems could greatly benefit from finely resolving the composition of the bulk pool, rather than distinguishing only between two broad fractions, allochthonous and autochthonous DOM (Pace et al., 2004) treated largely as black boxes. For instance, DOM optical properties such as fluorescence intensities of a set of fluorophores can give insights into DOM quality, and also facilitate the quantitative assessment of different compounds contributing to the DOM pool (Phong & Hur, 2015; Stedmon & Markager, 2005). Moreover, methodological advances in mass spectrometry enable analyses of organic matter at ultrahigh resolution (Dittmar et al., 2008; María et al., 2017), yielding compositional fingerprints composed of many hundreds to thousands of compounds. Although the scope for extracting quantitative information by this mass spectrometric approach remains limited at present, it is clear that both this approach and fluorescence-based DOM analyses offer unprecedented opportunities, particularly in combination, to open the black box of DOM in aquatic ecosystems (Riedel et al., 2016).

We use the concept of the “ecosystem metabolome” as a framework for such analyses (Danczak et al., 2020; Muscarella et al., 2019). In analogy to the metabolome of individual organisms, the “ecosystem metabolome” represents the entire DOM pool in an ecosystem. The rationale is, first, that ecosystems and

organisms, despite all differences, share important basic properties, including boundaries to an outside world and component integration (Tansley, 1939). More important, much like metabolic processes in cells, all biological, chemical, and physical processes in ecosystems leading to the consumption or production of organic compounds leave imprints on the DOM pool. That pool, in turn, encapsulates information on past transformation processes. Consequently, an ecosystem metabolome approach underlines the dynamic nature of DOM and its potential to infer past biogeochemical transformations. In analogy, human body samples such as saliva are used to diagnose disease based on metabolic fingerprints, even when understanding of individual metabolite behavior is limited (Sugimoto et al., 2010). Similarly, DOM samples from lakes may be useful to identify environmental pressures affecting lake ecosystem functioning.

It could also be worthwhile exploring aggregate characteristics of the DOM pool, in addition to DOM composition. For example, aggregate properties such as structural and functional chemical diversity (Mentges et al., 2017) or compositional turnover can be inferred from highly resolved, temporally repeated analyses of the ecosystem metabolome. For example, photodegradation of complex humic substances creates molecular signatures by removing and/or producing specific molecules (Stubbins et al., 2010), thus simultaneously affecting chemical composition and diversity of the metabolites that constitute the ecosystem metabolome (Mentges et al., 2017). Photodegradation increases molecular diversity because large aromatic compounds are cleaved into smaller entities (Riedel et al., 2016), and those smaller compounds, along with organic matter freshly produced by autotrophs, can be metabolized by heterotrophic microbes to generate yet a new set of metabolites (Cory & Kling, 2018). Although it generally remains challenging to disentangle which compounds originate from which process in complex natural environments, recent analytical progress (Dittmar et al., 2008) has shown that photodegradation affects overall DOM composition in aquatic ecosystems (Dittmar et al., 2007; Riedel et al., 2016; Stubbins et al., 2010).

In the present study, we explored whether qualitative and quantitative information derived from fluorescence signals and high-resolution mass spectrometry of DOM can inform about effects of nutrient enrichment and cDOM supply on lake ecosystem metabolomes. The underlying idea is that information contained in the composition, dynamics and properties of DOM can help to recover the effects of nutrients and cDOM on lake ecosystems. We performed a photodegradation assay in the laboratory and a large-scale enclosure experiment in the field, complemented by the analysis of an observational data set of 109 lakes distributed across Sweden. The goal of the laboratory experiment was to characterize the “ecosystem metabolome” resulting from photodegradation as an example of a specific DOM transformation process. The objective of the enclosure experiment was to test whether different metabolic processes can be disentangled, and the field data served to assess whether the patterns observed under controlled conditions in the experiments can be tracked in natural environments.

## 2. Materials and Methods

### 2.1. Experimental Design

The enclosure experiment was performed during summer 2015 in Lake Stechlin an oligo-mesotrophic clear-water lake in northeastern Germany (53°08'35.8"N 13°01'41.0"E). We used 21 large-scale enclosures ([www.lake-lab.de](http://www.lake-lab.de)) extending into the natural sediment at depths ranging from 16.3 to 20.5 m (mean = 18.4 m, SD = 1.4 m) and with a diameter of 9 m. Before starting the experiment, the water from the enclosures was exchanged with lake water in two steps by using impeller pumps (Lovara Domo 10 T/B SG, Xylem Innovative Systems GmbH) that have minimal damaging effects on plankton (Nejstgaard et al., 2006). Water below the thermocline at about 7 m depth was exchanged first before the process with the surface water was replaced. Further details on the LakeLab are given in Giling et al. (2017).

We experimentally mimicked brownification and nutrient enrichment by adding HuminFeed<sup>®</sup> (HuminT-ech, Grevenbroich, Germany) as a highly recalcitrant source of cDOM, nitrogen (N) as ammonium nitrate and phosphorus (P) as 85% phosphoric acid. HuminFeed<sup>®</sup> is a highly soluble alkaline extract of leonardite used commercially as feedstuff additive (e.g., Minguez et al., 2019). The N:P ratio reproduced the measured ratio of bioavailable N and total P in the lake (16:1 on a molar basis). To reproduce a range of browning and nutrient conditions, three cDOM levels (no addition, addition of 0.6 and 1.2 mg C L<sup>-1</sup>) were crossed with a 7-level nutrient gradient (no addition, addition of 1, 4, 9, 16, 25, and 36 μg P L<sup>-1</sup>). Thus, we used 21

individual enclosures in a nonreplicated gradient design to maximize the diversity of metabolites produced by potentially nonlinear responses of organisms to environmental stressors (Bergström & Karlsson, 2019; Kreyling et al., 2018). Measurements made before and after the addition indicated that the added cDOM had minimal effects on the intended nutrient gradient (13.4  $\mu\text{g N}$  and 0.58  $\mu\text{g P}$  per mg of HuminFeed<sup>®</sup>).

Once a week, integrated samples of epilimnetic water (0–7 m depth) were collected by hose samplers and filled in clean 20-L carboys. Cleaning involved rinsing of the carboys with 0.01 M HCl and de-ionized water and drip-drying overnight prior to usage. The collected water samples were transported to the laboratory where they were processed within one hour after sampling by filtering one liter from each enclosure through pre-combusted (4 h at 450°C) GF75 filters (Advantec, nominal pore size of 0.3  $\mu\text{m}$ ) at low pressure. Samples were taken over a 6-week period (June 10, 2015 to July 21, 2015) after the initial browning and nutrient pulse. Measurements made before and two weeks after the pulse were limited to optical properties and environmental variables (see below and Figure S1).

## 2.2. Environmental Variables

An automated multi-probe system (YSI Inc.; LI-COR Inc.) deployed in each enclosure recorded depth profiles (0.5 m steps) of water temperature (YSI 6560), pH (YSI 6579), dissolved  $\text{O}_2$  concentration (YSI 6150) and photosynthetically active radiation (PAR) (Li 193) every hour. The reported values represent the mean of the first 7 m (minimum mixed surface layer throughout the experiment) at the time of sampling (9:00–10:00 a.m.). The light extinction coefficient from 0 to 4 m was calculated by regressing log PAR over depth. Chlorophyll-*a*, total nitrogen and total phosphorus concentrations were determined according to ISO procedures (ISO 2944:2010, ISO 15681:2003, ISO 10260:1992) using a spectrophotometer (Hitachi U2900) or a FIA analyzer (FIA-System, MLE Dresden). The DOC concentration was measured by high temperature catalytic oxidation using a TOC-V analyzer (Shimadzu). More information on environmental variables are available in the supporting information.

## 2.3. Photodegradation of cDOM

To isolate one specific source process of DOM conversion, we conducted a laboratory experiment targeting the photodegradation of our model cDOM (HuminFeed<sup>®</sup>). The experiment was performed with water from the enclosure that received the highest load of cDOM (1.2  $\text{mg C L}^{-1}$ ) and nutrients (36  $\mu\text{g P L}^{-1}$ ) in the enclosure experiment. The water was passed through 0.22  $\mu\text{m}$  filters (Millipore Sterivex, Merck) and filled into 31 acid-washed and pre-combusted (4 h, 450°C) 250 mL Erlenmeyer glass flasks. Sterile filtration and aseptic procedures served to minimize microbial DOM degradation. Three flasks serving as dark controls were wrapped in aluminum foil and three blank controls contained Milli-Q water only. All flasks were exposed to direct sunlight for 28 days. The borosilicate glass we used effectively blocked a large part of UV radiation (e.g., Gautam & Yadav, 2013), but to a lesser extent than along the 7-m depth gradient in the mixed surface layer of the lake. Three flasks were harvested every two days during the first week and then at weekly intervals for a total of four weeks. Control flasks were sampled initially, after 14 days and at the end of the experiment. DOC concentration and DOM optical properties and molecular composition were determined as described below.

## 2.4. Optical Properties and PARAFAC Modeling

Absorbance and fluorescence measurements can broadly inform about optical properties and thus molecular formulas of DOM constituents (e.g., Murphy et al., 2008). Absorbance spectra ranging from 190 to 800 nm at 1-nm resolution were determined for samples from the enclosure and photodegradation experiment by using a UV-VIS spectrophotometer (Hitachi U2900). Milli-Q water was used as a blank. Excitation-emission matrices (EEMs) were generated using a fluorescence spectrophotometer (Hitachi F-7000), with excitation wavelengths ranging from 220 to 450 nm at 5-nm increments, and emission wavelengths ranging from 230 to 600 nm at 2-nm increments. EEMs were blank-corrected using Milli-Q water, corrected for inner filter effects by the absorbance-based method (Christmann et al., 1980; Murphy et al., 2013) and expressed in Raman units. Before PARAFAC, EEMs were normalized to the total fluorescence intensity, and data in the primary and secondary Rayleigh and Raman scatter regions were deleted and linearly

interpolated. PARAFAC modeling was performed with the drEEM toolbox (Murphy et al., 2013) in MatLab (7.11.0) using all samples collected in the 21 enclosures and the adjacent lake. There were 216 samples in total. The PARAFAC model was fitted with multiple random starts and half-split validated following the drEEM pipeline (Murphy et al., 2013). The concentration components ( $F_{\max}$  values) of the PARAFAC model were transformed back to Raman units by multiplication with total fluorescence intensity. The PARAFAC model was also fitted to EEMs obtained from the laboratory photodegradation assay. The data were expressed in Raman units as a quantitative measure, thus changes in fluorescence intensity indicate actual increases or decreases in a given fluorophore identified as a PARAFAC component (Murphy et al., 2013).

### 2.5. DOM Molecular Composition and Diversity

We characterized DOM at the molecular level by using high-resolution mass spectrometry. Volumes of 250 mL filtrate were acidified to pH 2 with 0.1 M HCl within <30 min after water collection. DOM was then extracted by solid-phase extraction using PPL cartridges (BondElut, Agilent) according to Dittmar et al. (2008). Extraction efficiencies ranged from 65% (clear-water enclosures) to 85% (addition of 1.2 mg C L<sup>-1</sup>). Extracts were adjusted to a final DOC concentration of 30 µg L<sup>-1</sup> in a 1:1 (v:v) mix of methanol and water (both ultrapure). After a last filtration step through 0.2 µm PTFE syringe filters, the extracts were injected at a rate of 120 µL h<sup>-1</sup> into a 15 Tesla ultrahigh resolution FT-ICR-MS (Solarix, Bruker Daltonics) in ESI-negative mode (Dittmar et al., 2008). The instrument was run in broadband mode with mass to charge ratios (m/z) ranging from 150 to 2,000. A total of 300 scans was obtained. No peaks were detected for m/z higher than 1,000. This means we retrieved neither small compounds <150 Da (the lower technical limit of the instrument) nor large compounds >1000 Da. Spectra were subject to internal mass calibration using a set of pre-defined ubiquitous sum formulas that have proved useful in freshwater studies (Bruker Daltonics Data Analysis 4.0 SP 3 software package). Mass lists at S/N > 1 were exported at 10<sup>-6</sup> Dalton precision. These relaxed export settings were followed by strict data processing rules following the pipeline established by del Campo et al. (2019). Briefly, after application of a method detection limit and alignment of spectra, molecular formulas were assigned to mean m/z values. Single-charged deprotonated ions and Cl-adducts were assumed for a maximum elemental combination of C<sub>100</sub>H<sub>250</sub>O<sub>80</sub>N<sub>4</sub>P<sub>2</sub>S<sub>2</sub> with a mass tolerance of 0.6 ppm and several restrictions imposed on elemental ratios. Unequivocal formula assignments were resolved by (i) applying a refined mass tolerance for frequent peaks with more accurately estimated mean masses, (ii) isotope confirmation, and (iii) assessment of homologous series. Further details are given in supporting information. A total of 3,143 sum formulas covering on average 68% of the total spectrum intensity were retrieved and grouped into pre-defined chemical groups (Lesaulnier et al., 2017; Šantl-Temkiv et al., 2013). DOM chemodiversity was expressed as Shannon diversity index (Shannon & Weaver, 1949) using relative intensities of assigned molecular formulas. The double-bond equivalent (DBE) and aromaticity index (AI) were calculated as described in Koch and Dittmar (2006) and Singer et al. (2012). Details about molecular formula assignment are given in supporting informations.

### 2.6. Application to Field Data

A published ultra-high-resolution DOM data set containing PARAFAC data (Kellerman, 2015; Kellerman et al., 2015) was used to test whether results from our experiments might be transferred to field settings. The field data set encompasses data from 109 clear and brown-water lakes distributed across Sweden. Mass spectrometric information in this data set to which no molecular formula was attributed were discarded.

### 2.7. Data Analysis

Figure 1 presents a schematic of the workflow of the data analysis based on fluorescence measurements and relative intensity data derived from FT-ICR-MS analyses. First (step 1 in Figure 1), we computed general additive models (GAM; Hastie & Tibshirani, 1990) describing the dynamics of each identified PARAFAC component for each cDOM level in the enclosure experiment as a smoothing function of sampling time (hereafter referred to as “Time”). Samples were grouped within cDOM treatments by using all data from the seven enclosures per cDOM level (which received different amounts of nutrients) at each sampling time.

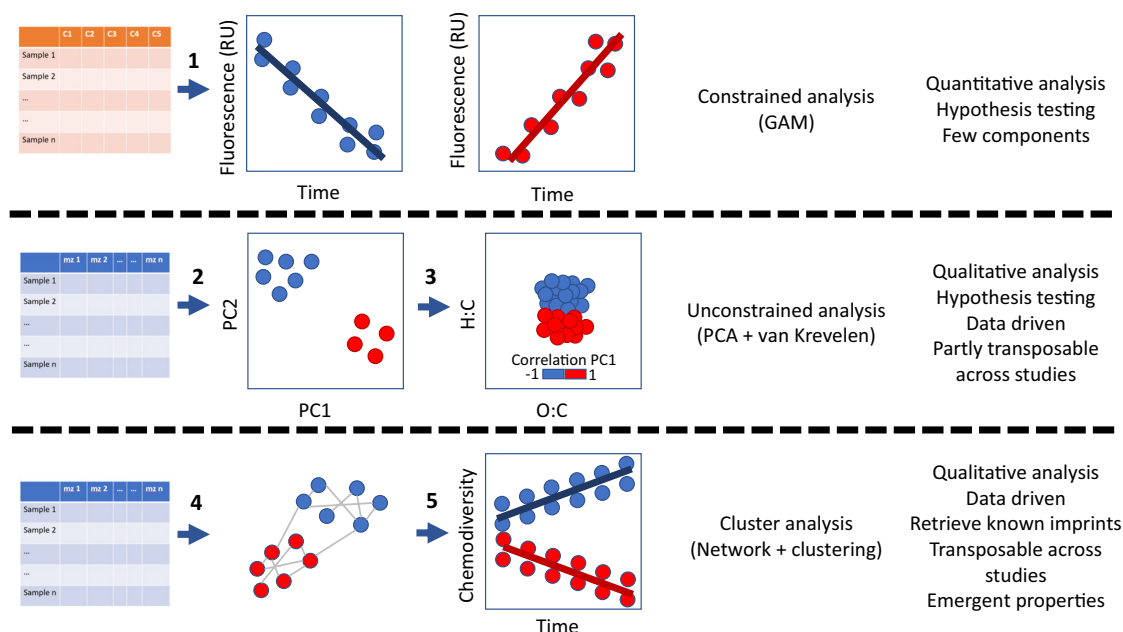


**Figure 1.** Workflow for analyzing lake ecosystem metabolomes. Arrows indicate pathways of data flow while numbers indicate the order in which analysis steps were performed. Pathways of quantitative and qualitative data flows are shown in orange and blue, respectively. **1:** General additive models (GAMs) to evaluate the dynamics of PARAFAC components. **2:** The centered-log ratio transformation of FT-ICR-MS data to reduce highly dimensional data on organic matter composition. **3:** Partial RDA to assess the dynamics of ecosystem metabolomes, with scores mapped onto van Krevelen space. **4:** A SPIEC-EASI co-variation network and subsequent clustering to separate metabolites based on their interactions into dominant clusters. **5:** van Krevelen plots produced for each cluster. **6:** Dynamics of cluster-specific Shannon diversity to be evaluated with GAMs.

For the highly dimensional, compositional FT-ICR-MS data, we used centered log ratio (clr) transformed intensities (step 2 in Figure 1) and multivariate statistics to reveal stressor effects. Given previous indications of a notable machine drift, we used a partial redundancy analysis (pRDA) using time of the mass spectrometric measurement as a constraint (Davies & Tso, 1982). Measurement time on the FT-ICR-MS was not available for the Swedish data set. Therefore, we performed a principal component analysis (PCA) on clr-transformed intensities. To locate molecular formulas associated with the two stressors in van Krevelen diagrams (e.g., Herzsprung et al., 2012; step 3 in Figure 1), we computed Spearman rank correlations between sample scores on the PC-axes of the pRDA and (i) the two experimental stressors, or (ii) clr-transformed intensities. Color coding of the molecular formulas shown in van Krevelen space was based on the strength of these correlations.

Viewing an “ecosystem metabolome” as a complex network of “metabolites” with connections of varying strengths, we used the sparse inverse covariation estimation for ecological association inference (spiec-EASI; Kurtz et al., 2015) to construct a metabolic network (step 4 in Figure 1). We used edges (i.e., connections between two nodes) to describe a DOM transformation process (Camacho et al., 2005; Jeong et al., 2000; Spirin et al., 2006). Thus, a positive edge was used to indicate that “metabolites” are supplied by a common source process such as photosynthesis, terrestrial input, or release by a particular organism. Conversely, a negative edge was considered an indication of DOM constituents being converted, as evidenced by decreases in substrate concentrations and concomitant increases in product concentrations. We retrieved clusters of metabolites from the network with the Glay method (Su et al., 2010) and the Fast-greedy algorithm (Clauset et al., 2004), and obtained information on the density of edges inside clusters using the NetworkAnalysier plugin for Cytoscape (Doncheva et al., 2012). In a follow-up step, we analyzed the identified metabolite clusters for differences in chemical composition and, by calculating the Shannon index for each cluster, in chemical diversity.

We evaluated differences in chemical composition by testing for differences in DBE and molecular weight of molecular formulas among clusters using robust ANOVA, a variant of classic ANOVA based on regression coefficients that are less influenced by outliers (packages *MASS* and *lmtest*; Hothorn et al., 2011; Ripley

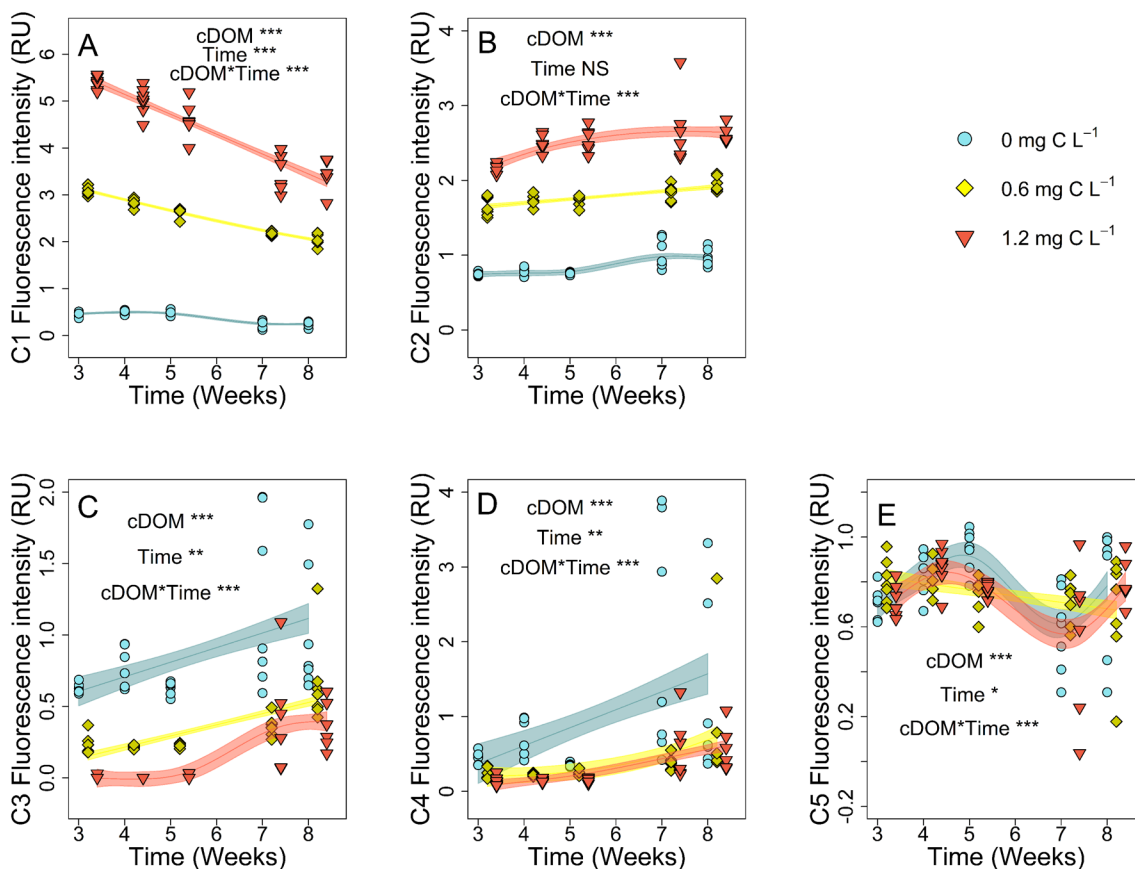


**Figure 2.** Dynamics of dominant dissolved organic matter (DOM) clusters revealed by PARAFAC. Data are expressed in Raman Units (RU). Blue dots represent clear-water enclosures, yellow diamonds, and red triangles represent enclosures receiving 0.6 and 1.2 mg C L<sup>-1</sup>, respectively. Lines and shaded areas represent GAM best fits and standard errors of the GAM models, respectively. (a and b) show humic-like PARAFAC components 1 and 2 while (c–e) show the protein-like PARAFAC components 3, 4 and 5. Results are only reported when the significance level for colored dissolved organic matter (cDOM) level, Time, s(Time) or their interaction was lower than  $P = 0.05$ . Three asterisks indicate  $P < 0.001$ . NS = not significant ( $p > 0.05$ ).

et al., 2019) and by testing for differences of formulas assigned to molecular categories (e.g., lipids, peptides) using a chi-squared test (see supporting information for details). For visualization, we plotted members of each cluster in van Krevelen space, with superimposed contour plots showing the density of compounds (step 5 in Figure 1). Differences in chemical diversity were analyzed using GAMs (step 6 in Figure 1). Unless stated otherwise, all statistical analyses were performed using the packages *gam* (T. Hastie, 2015) and *vegan* (Oksanen et al., 2013) in R 3.5.1 (R Core team, 2017).

### 3. Results

#### 3.1. Dynamics of DOM Composition Inferred from Fluorescence Signatures

We identified five distinct PARAFAC components, two humic-like (C1 and C2) and three protein-like components (C3, C4 and C5) (supporting information). The two humic-like components, C1 and C2, showed opposite trends in the “brown” enclosures with added cDOM (Figures 2a and 2b). C1 linearly decreased in importance over time whereas C2 increased. As a result, C1 and C2 were negatively correlated in the two brown enclosures receiving cDOM at medium ( $\rho = -0.63$ ,  $p < 0.01$ ) and high level ( $\rho = -0.46$ ,  $p < 0.01$ ). In the clear-water enclosures, the abundance of both components remained constantly low throughout the experiment (Figures 2a and 2b). This pattern contrasts with the occurrence of two of the protein-like components, C3 and C4. Both were abundant in the clear-water enclosures from the beginning of the experiment and increased further toward the end, but they were initially rare in the brown enclosures and only increased in abundance six weeks after the cDOM addition (Figures 2c and 2d). Another protein-like

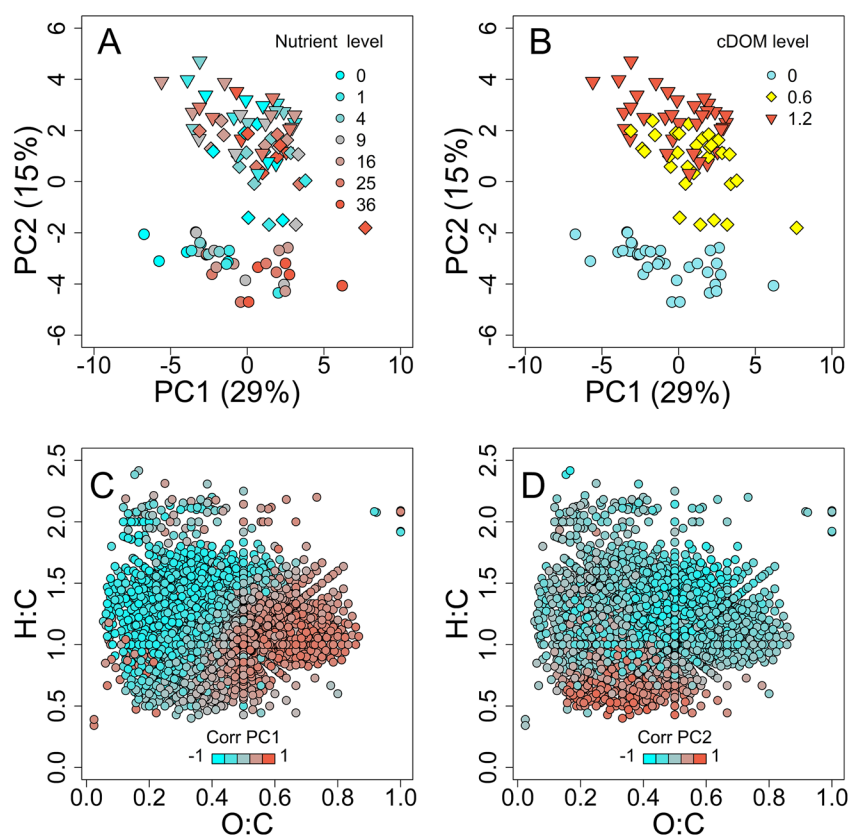


**Figure 3.** Effects of browning and nutrient enrichment on lake ecosystem metabolomes. (a and b) Partial redundancy analyses performed on clr-transformed intensities of all metabolites identified in an enclosure experiment to assess effects of browning and nutrient enrichment on lake ecosystem metabolomes. Shown are the first two unconstrained axes associated with the two stressors, whereas the constrained axis is considered instrument-borne bias. Dots represent clear-water enclosures, and diamonds and triangles represent enclosures receiving 0.6 and 1.2 mg C L<sup>-1</sup> of colored dissolved organic matter (cDOM), respectively. (c and d) van Krevelen diagrams depicting Spearman correlation coefficients between clr-transformed intensities of all assigned metabolites and sample scores on the principal component axes in panels (a) and (b).

component, C5, showed significant differences between clear-water and brown enclosures but clear monotonic trends did not emerge from the data (Figure 2e).

### 3.2. Dynamics of DOM Composition Inferred from FT-ICR-MS

Partial ordination of FT-ICR-MS data adjusted for instrumental drift revealed that the first principal component (29.4%) was positively related to the level of nutrient addition ( $\rho = 0.24$ ,  $p < 0.05$ ), whereas the second principal component (15.0%) was negatively related to the quantity of cDOM ( $\rho = -0.87$ ,  $p < 0.001$ ) (Figures 3a and 3b). Mapping the first two axes into van Krevelen space facilitated identifying metabolites driving the overall pattern (Figures 3c and 3d). The O:C ratios correlated positively with PC1, suggesting oxygen-rich metabolites were associated with elevated nutrient supply, and vice versa for oxygen-poor metabolites. The H:C ratios correlated negatively with PC2, suggesting H-unsaturated metabolites were positively associated with the addition of cDOM. In contrast, metabolites with high H:C ratios predominantly appeared in enclosures without added cDOM.

### 3.3. Molecular Interactions in the DOM Pool

Our network analysis of metabolites in the DOM pool identified by FT-ICR-MS revealed 3,143 nodes (i.e., metabolites) and 57,614 edges (i.e., connections). Five distinct clusters of metabolites could be discriminated (Figure 4a). The first cluster contained 57.6% of all metabolites, and the second and third largest clusters



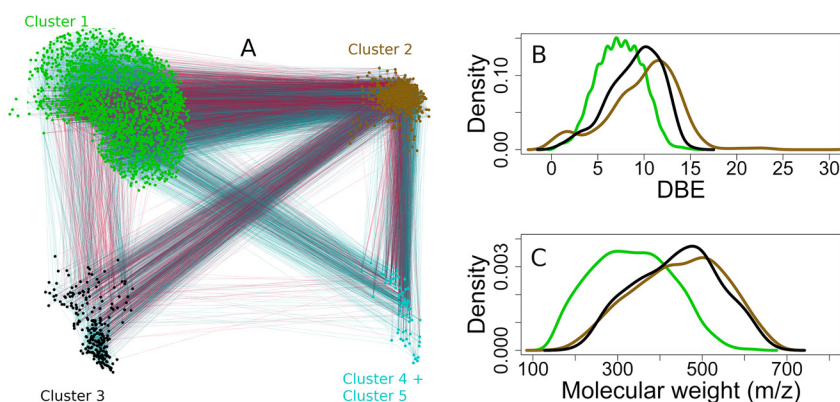


**Figure 4.** Dissolved organic matter (DOM) molecular interaction network and cluster characterization. (a) Spiec-EASI network with each dot representing a molecular formula and each edge a putative process. Nodes are colored according to Glay clusters, positive and negative edges are represented in turquoise and red, respectively. Clusters 1, 2, and 3 are represented in green, brown and black, respectively. (b) Kernel density plots of the molecular mass for all molecular formulas present in Clusters 1, 2, and 3. (c) Kernel density plots of double-bond equivalents (DBE) for all molecular formulas in Clusters 1, 2, and 3.

accounted for an additional 40.2%. The last two clusters (4 and 5) together only represented 2.3% (Figure 4, Table 1). Thus, we focus on the three main clusters (1–3) for deeper analyses. There were major differences in chemical properties among members of the three main clusters (Figures 4b, 4c and 5): most compounds in Cluster 1 showed greater saturation (mean DBE = 7.4 SD = 2.4) and had a low-molecular weight (mean  $m/z$  = 332.9, SD = 94.0) and little P (i.e., only 0.83% of all molecules in this cluster contained P), although N was not particularly low (Table 1).

In contrast to Cluster 1, Clusters 2 and 3 typically contained unsaturated molecules (mean DBE = 9.90 and 8.98, SD = 4.11 and 2.87, for Cluster 2 and 3, respectively) that had a relatively high molecular weight (mean  $m/z$  = 447.6 and 437.9, SD = 105.9 and 98.0 for Clusters 2 and 3, respectively; Table 1). Both DBE and molecular weight were significantly different among the three main clusters (robust ANOVA,  $P < 0.01$ ; see Figures 4b and 4c for differences in distributions). In addition, these clusters differed with respect to the proportion of metabolites in the different molecular categories ( $X^2 = 360$ ,  $df = 22$ ,  $p < 0.001$ , Figure 5) and the density of edges (robust ANOVA,  $P < 0.01$ ). Specifically, Cluster 1 had the highest proportion of highly unsaturated compounds with an O:C lower than 0.5 and clustered with Lake Stechlin and an enclosure supplemented with N and P only (Figures 5a and 5b). Cluster 2 had a higher proportion of polyphenolic compounds, black carbon, and highly unsaturated oxidized compounds (O:C > 0.5), similar to HuminFeed (Figures 5a and 5c). Cluster 3 had the highest proportion of highly unsaturated oxidized compounds (O:C > 5), which constituted the majority (>50%) of the compounds in Cluster 3 (Figures 5a and 5d).

Cluster 1 contained metabolites showing weaker relationships with one another than those in Clusters 2 and 3 (network density = 1, 5.5% and 4.5% for Clusters 1, 2, and 3, respectively). Furthermore, 97% of the

**Table 1**  
 Characteristics of the Five Main Clusters Identified in Lake Water

Cluster	Number of nodes	Density edges	DBE <sup>a</sup> mean (SD)	C/N Mean (SD)	C/P mean (SD)	Nodes with N (%)	Nodes with P (%)	$m/z$ mean (SD)	Neactive - positive edges	Chemodiversity mean (SD)
1	1809	0.010	7.4 (2.4)	12.1 (4.7)	13.2 (5.1)	665 (37%)	15 (1%)	333 (94)	3.4–96.6	4.51 (0.05)
2	1021	0.055	9.9 (4.1)	11.8 (5.9)	15.2 (6.3)	210 (21%)	77 (8%)	448 (106)	44.3–55.7	5.99 (0.05)
3	241	0.045	9.0 (2.9)	13.6 (6.3)	12.4 (6.4)	92 (38%)	9 (4%)	438 (98)	2.2–97.8	6.65 (0.06)
4	63	0.080	8.2 (2.3)	20.6 (4.7)	20 (–)	13 (21%)	1 (2%)	457 (91)	4.4–95.7	3.99 (0.08)
5	8	0.643	7.6 (1.3)	0	0	0 (0%)	0	439 (71)	38.9–61.1	1.98 (0.35)

<sup>a</sup>DBE = Double-Bond Equivalent,  $m/z$  = mass to charge.

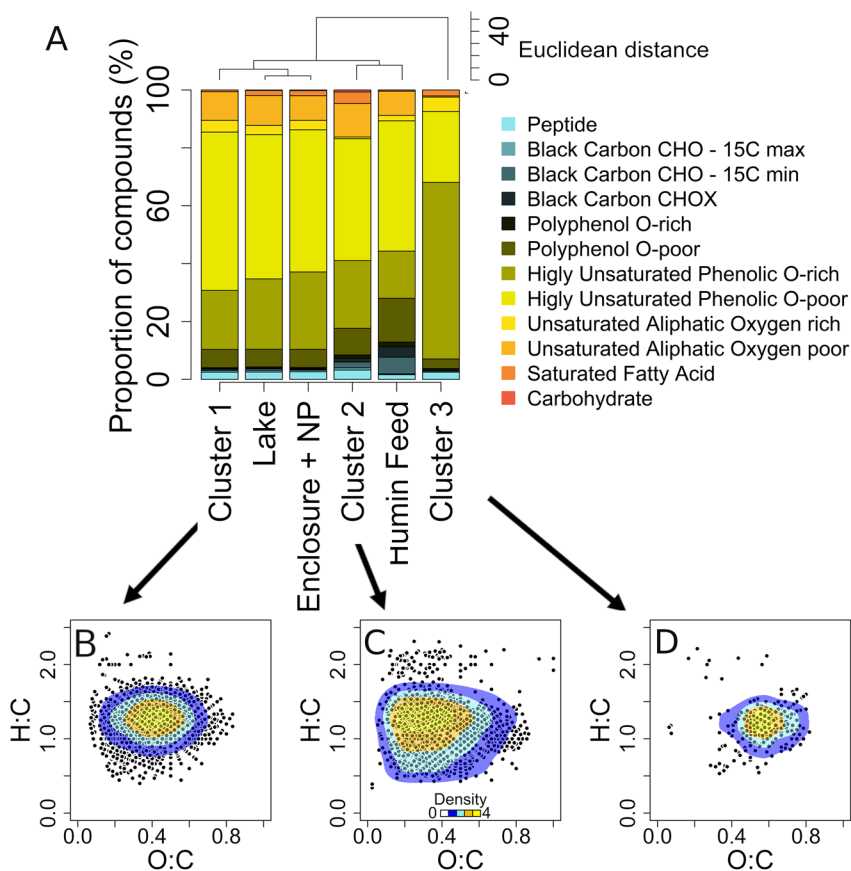


**Figure 5.** Differences in molecular composition among clusters. (a) Stacked bar chart depicting differences among clusters with regard to molecular categories. (b–d) van Krevelen diagrams of molecular formulas in Clusters 1, 2, and 3. Each gray dot represents a molecular formula, colored contours show densities of molecules in chemical space defined by O:C and H:C ratios. Black carbon molecular formulas are distinguished into those with 15 or more, and those with fewer than 15 carbon atoms.

compounds in Cluster 1% and 98% of the compounds in Cluster 3 shared positive edges, while this proportion was only 56% for Cluster 2 (Table 1). The last two clusters were very small in terms of metabolite numbers (Cluster 4 and 5) and were similar to Clusters 2 and 3 with a high proportion of unsaturated compounds of high molecular weight. DOM Shannon diversity diverged among the three main clusters (Figure 6). In the brown enclosures, the Shannon index of Clusters 1 and 2 increased over time, whereas it first decreased in Cluster 3 to reach a minimum after four weeks. In clear-water enclosures, Shannon diversity fluctuated but showed no clear overall trend for any of the three clusters.

### 3.4. Photodegradation of DOM Compounds

Most (99.7%) of the metabolites identified in water samples collected during the enclosure experiment were retrieved in the photodegradation assay. Compounds were homogeneously distributed in the van Krevelen space and encompassed a wide range of compounds (Figure 7a). We found four out of five PARAFAC components (Figure 7b). Similar to the enclosures receiving cDOM, the PARAFAC component C1 strongly declined initially before it increased again toward the end, whereas component C2 initially increased and then leveled off (Figure 7b). PARAFAC component C3 was not found in the photodegradation experiment conducted in Erlenmeyer flasks. C4 and C5 decreased during the first week, and then remained at a constant level until they increased again during the last week of incubation. Shannon diversity showed a unimodal pattern characterized by an initial sharp increase followed by a more gradual decline (Figure 7c). The first axis of a PCA performed on the clr intensities of the identified metabolites was positively correlated with elapsed time (i.e., exposure time of DOM to light) (Figure 7d). Mapping this PC1 onto the van Krevelen

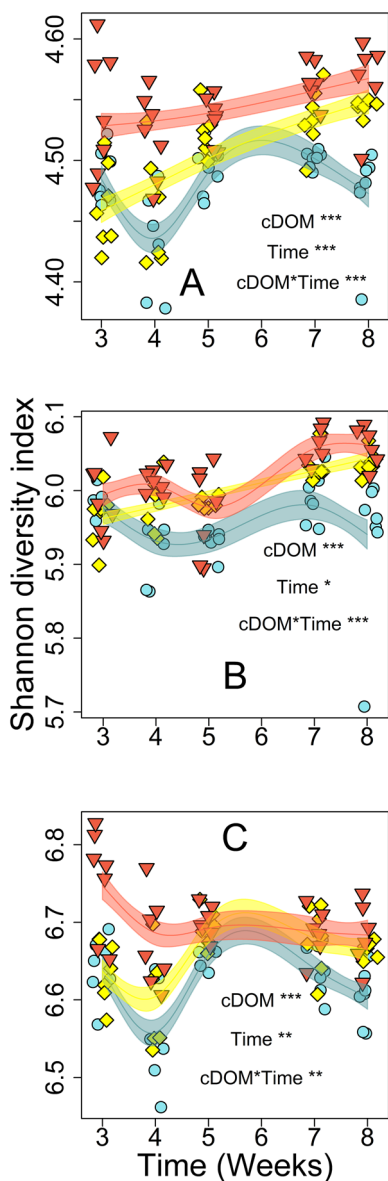


**Figure 6.** Dynamics of molecular diversity. Dynamics of Shannon diversity for Clusters 1 (a), 2 (b) and 3 (c). Blue dots represent clear-water enclosures, yellow diamonds and red triangles represent enclosures receiving 0.6 and 1.2 mg C L<sup>-1</sup> of colored dissolved organic matter (cDOM), respectively. Lines and shaded areas represent best fits and standard errors of general additive models (GAMs).

from traditional tests of effects on DOM composition in that it seeks to infer causes (environmental drivers) from observed effects (i.e., the characteristics of the ecosystem metabolome) rather than the reverse. One reason for this choice is the multivariate nature of DOM data, which often results in effects being hidden by compositional artifacts inherent in high-resolution methods (Pesenson et al., 2015). A consequence is that constrained hypothesis-testing analyses are often successful even when obvious hypothesis-related variation in unconstrained analyses is lacking, and this leads to differences in ordination patterns between constrained and unconstrained multivariate analyses.

space showed compounds with low O:C ratios to be more prone to photodegradation than compounds with high O:C ratios, reflecting a greater relative abundance of compounds rich in O at the end of the experiment (Figure 7e).

### 3.5. Application to Field Data

The first axis (PC1) of our principal component analysis performed on clr-transformed intensities of all compounds identified in the field data set was positively correlated ( $p < 0.05$ ) with UV absorbance of the water (Figure 8a) and strongly related to a compositional change of low H:C compounds in brown water (Figure 8b). This outcome is consistent with the pattern shown in the original report by Kellerman et al. (2015). Network analysis of the DOM pool revealed 2,873 nodes and 96,291 edges (Figure 9). Due to the low number of metabolites in Cluster 4 (8 in total), and their chemical similarity to those of Cluster 3, we combined both to facilitate the graphical representation (Figure 9, Table 2). Similar to the results from our enclosure experiment, one of the clusters (i.e., Cluster 1) had a lower density of edges, a lower DBE and compounds with lower molecular weights (Table 2) than Clusters 2 and 3 (Table 2). These three clusters were also distinct with regard to the proportion of metabolites in the different molecular groups ( $X^2 = 156.7$ ,  $df = 22$ ,  $p < 0.001$ , Figure S8). They differed primarily in their proportions of highly unsaturated oxidized compounds (O:C > 0.5, Figure S8), black carbon and polyphenols. Moreover, we noted similarities with clusters in samples from the enclosure experiment (Figure S8). Only PARAFAC component 6, described as a protein-like component in the original report by Kellerman et al (2015), was positively correlated with metabolite diversity in Cluster 2 (Spearman correlation,  $\rho = 0.23$ ,  $p < 0.05$ ). Conversely, PARAFAC components 1 to 5 were positively correlated with the diversity of compounds in Clusters 1 (Spearman correlation  $\rho = 0.36$ ,  $p < 0.05$  and  $\rho = 0.34$ ,  $p < 0.05$ , respectively) and PARAFAC components 2 to 5 were positively correlated with the diversity of compounds in Cluster 3 (Spearman correlation  $\rho = 0.27$ ,  $p < 0.05$  and  $\rho = 0.28$ ,  $p < 0.05$ , respectively).

## 4. Discussion

Our results illustrate that imprints of environmental drivers such as brownification and—to a lesser extent—nutrient enrichment can be identified through analyzing metabolites in the DOM pool of lake water. The five metabolite and fluorophore clusters identified in our enclosure experiment related to cDOM or nutrient amendment, suggesting that information on the “ecosystem metabolome” can point to environmental stressors in lakes. Our approach to elucidate such DOM signatures differs

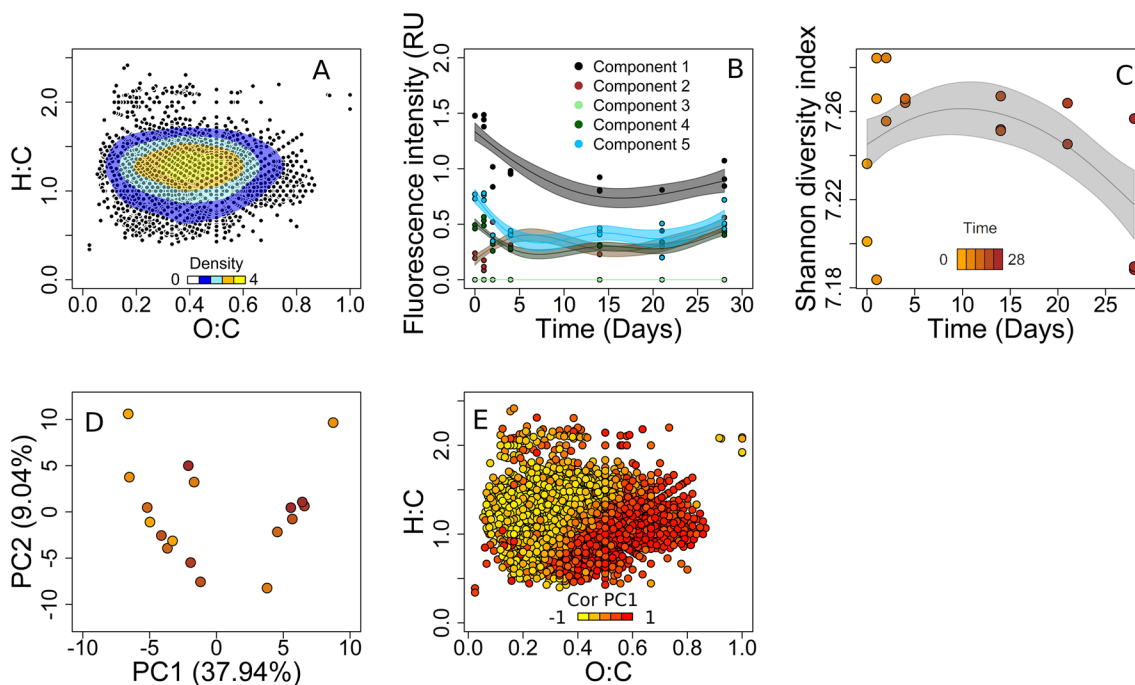


**Figure 7.** Characteristics and evolution of compounds exposed to sunlight. (a) van Krevelen diagram of all molecular formulas identified in a photodegradation assay in sterile conditions. Colored contours show densities of molecules in chemical space defined by O:C and H:C ratios. (b) General additive models (GAMs) representing the evolution of all PARAFAC components in the photodegradation assay. Lines and shaded areas represent GAM best fits and standard errors of the models. (c) GAM depicting the dynamics of Shannon diversity in the photodegradation assay, with the color of dots distinguishing sampling times. (d) First two unconstrained axes of a partial redundancy analysis displaying compositional changes due to photodegradation. Colors correspond to the incubation time as in panel (c) and (e). (e) Spearman rank correlation between metabolite intensities and the first principal component axis in panel (d). Compounds degraded or produced as a result of light exposure occupy the yellow and red ends of the color gradient, respectively.

#### 4.1. DOM Proxies of Browning and Nutrient Enrichment

The increase in two humic-like DOM components, C1 and C2, that we observed following experimental browning, in contrast to clear-water enclosures, corroborates previous studies assessing effects of lake brownification (Brothers et al., 2014; Roulet & Moore, 2006). The opposite dynamics of C1 and C2 suggest coupled photodegradation and photo-production processes, as previously noted (Attemeyer et al., 2015;

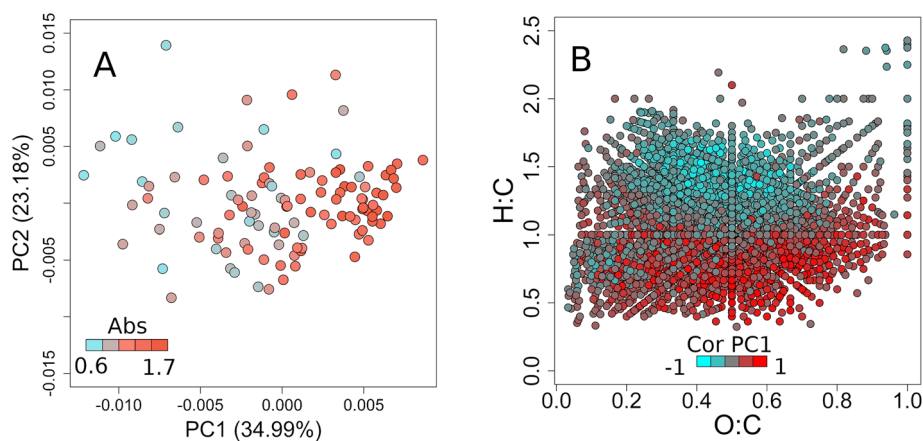


**Figure 8.** Changes in dissolved organic matter (DOM) composition in 109 Swedish lakes. (a) Principal component analysis performed on clr-transformed intensities of metabolites. (b) van Krevelen diagrams with colors showing Spearman correlations between clr-transformed intensities and sample scores on the first principal component axis in panel (a).

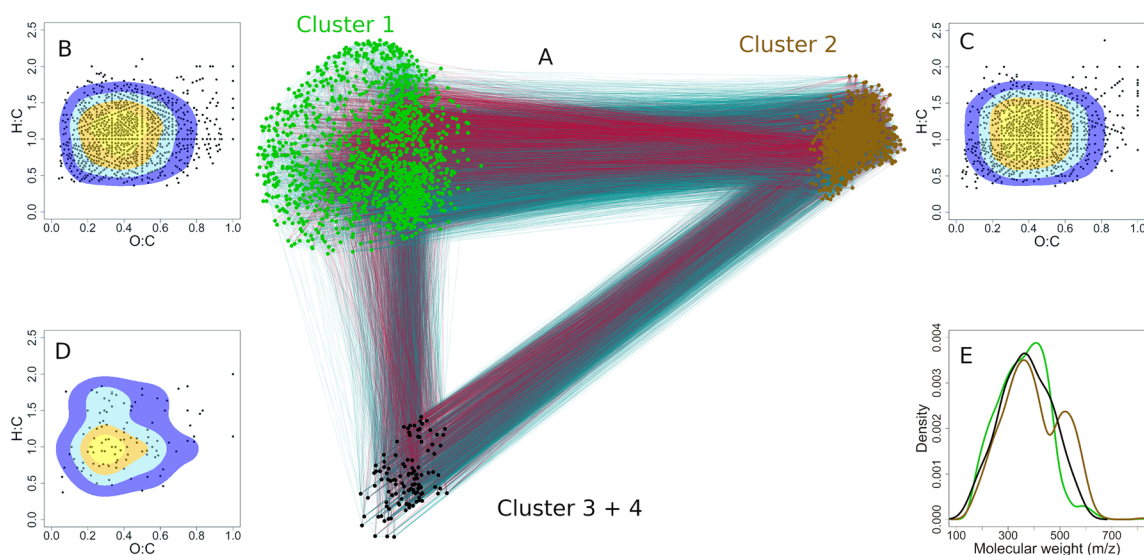


**Figure 9.** Conditional independence network partitioning the metabolome of 109 Swedish lakes. (a) Spiec-EASI network where each dot represents a molecular formula and each edge a process. Nodes are colored according to Glay clusters, positive and negative edges are represented in turquoise and red, respectively. Clusters 1, 2, and 3 are represented in green, brown and black, respectively. Panels (b–d) van Krevelen diagrams of molecular formulas identified in the data set and present in Clusters 1, 2, and 3, respectively. Colors indicate the density of metabolites in each cluster. (e) Kernel density plots of the molecular mass for all molecular formulas in Clusters 1, 2, and 3.

Spencer et al., 2009; Stubbins et al., 2010). This conclusion is further supported by the decrease in C1 we observed in the photodegradation assay in Erlenmeyer flasks, even though C2 increased only slightly in that assay, possibly due to concomitant degradation in the rather intensely irradiated bottle environment.

Browning also strongly increased light extinction, which directly affects primary production (Karlsson et al., 2009). Therefore, the marked decline in protein-like fluorophores observed in our enclosures receiving cDOM is likely due to reduced primary production caused by light-limitation. When subsequent photodegradation of cDOM gradually alleviated this limitation, C3 and C4 could eventually recover in the brown enclosures. This suggests that the dynamics of C3 and C4 were associated with autotrophic production, either directly as a result of algal carbon exudation, or indirectly, for instance due to metabolic byproducts released by consumers that benefit from an increased resource base. Thus, PARAFAC modeling proved valuable in our experiment to disentangle allochthonous and autochthonous DOM and might well be used to make functional inferences with regard to terrestrial inputs or aquatic primary production from DOM dynamics (Osburn & Stedmon, 2011; Stedmon et al., 2007). However, the evaluation of nutrient addition effects by PARAFAC modeling could still be hampered by “invisible” compounds that do not absorb light in the UV-visible range and thus cannot be detected by standard optical methods (Pereira et al., 2014).

#### 4.2. Compositional Responses of DOM to Browning and Nutrient Enrichment

The highly dimensional data set obtained by FT-ICR-MS contained thousands of distinguishable compounds. Compared to a handful of fluorophores, it may thus provide a much refined representation of the “ecosystem metabolome” defined here conceptually as all “metabolites” present in an ecosystem. This

**Table 2**  
*Characteristics of the Three Main Clusters Identified in the Swedish Lake Data Set*

Cluster	Nodes	Density edges	DBE mean (SD)	H/C mean (SD)	O/C mean (SD)	m/z mean (SD)	Negative – Positive edges (%)
1	1478	0.019	8.4 (3.3)	1.2 (0.3)	0.46 (0.17)	356.8 (95.3)	26.7–73.3
2	1282	0.051	10.2 (3.8)	1.1 (0.3)	0.45 (0.19)	394.7 (113.0)	45.1–54.9
3	105	0.073	9.1 (3.5)	1.1 (0.3)	0.45 (0.18)	363.3 (98.1)	39.3–60.8

extends the simple, albeit often useful and commonly adopted, distinction between allochthonous and autochthonous organic matter.

The low H:C region in the van Krevelen space is not uniquely occupied by humic matter (Koch & Dittmar, 2006) but also by highly unsaturated phenolic compounds. Similarly, the high O:C ratio region contains various compounds, such as carbohydrates, other than those associated with nutrient enrichment (e.g., Brockman et al., 2018; D'Andrilli et al., 2015). However, metabolites with a low H:C ratio have previously been observed to be abundant in various humic freshwater systems (Herzsprung et al., 2017; Zherebker et al., 2016), and metabolites characterized by high O:C ratios (e.g., carbohydrates) are usually more abundant in eutrophic water bodies (Lusk & Toor, 2016b, 2016a; Zhou et al., 2018). Thus, our data suggest that DOM signatures in lakes analyzed by FT-ICR-MS potentially inform about impacts on lakes by environmental drivers such as browning by cDOM and nutrient supply. Accordingly, the brown and clear-water enclosures in our experiment receiving varying amounts of nutrients were separated along PC2 of our PCA based on browning levels and along PC1 based on nutrient levels, together accounting for almost half of the total variation in the data set.

### 4.3. Assigning Source Processes to Constituents of the Ecosystem Metabolome

Most metabolites identified in our analysis grouped into three main clusters, which were defined by shared dynamics related to processes such as primary production, allochthonous organic matter supply, photodegradation, and microbial decomposition. These clusters differed in chemical composition, diversity and connection among metabolites. Low-molecular weight molecules are considered autochthonous (Bracchini et al., 2010; Brandão et al., 2018; Fasching et al., 2014), whereas high-molecular weight compounds tend to be of allochthonous (terrestrial) origin. Accordingly, we attributed a lake origin to the low-molecular weight compounds comprising Cluster 1. Clusters 2 and 3, in contrast, appeared to share a terrestrial origin, since Cluster 3 shared similarities with photodegraded compounds (Figure S6), and metabolites in Cluster 2 were associated with our model cDOM (Figure 5), HuminFeed<sup>®</sup>, originally added to the enclosures. Thus, our network analysis identified three major processes involved in DOM dynamics, each of them reflected in a different cluster of the ecosystem metabolome.

Such a classification allows sorting molecular formulas based on their origin and reactivity. For instance, compounds of Cluster 3 presumably derived from the cDOM we added (informs about origin) and were photodegraded (informs about reactivity). These have the highest proportion of oxidized compounds (Stubbins et al., 2010) and are quite distinct in this regard from Clusters 1 and 2 (Figures 5, S6, and S8). These two in turn each reflect a distinct origin again: autochthonous production resembling the lake metabolome and added cDOM, respectively, with distinct molecular group distributions. Freshly produced autochthonous DOM compounds tend to be more oxidized than lignin-derived compounds (Maizel et al., 2017), yet there is large overlap in van Krevelen space between Clusters 1 and 2. It is important to note that our inference of molecule clusters is based on detectable relationships (edges in the network) rather than elemental composition. The approach also detects aggregate properties, such as measures of connectedness between molecular formulas, and is capable of distinguishing functionally different formulas positioned in the same region of van Krevelen diagrams (Figures 5 and S8). However, like other analyses, our approach is limited by the analytical window defined by limitations in extraction, ionization and mass-spectrometric detection. Moreover, the ionization efficiency of compounds depends on the richness and abundances of other compounds in the sample matrix. The latter may have implications when inferring a network structure from samples of different origins, but unlikely affected our results where samples shared the same background matrix.

### 4.4. DOM Composition and Diversity

Allochthonous DOM represents the largest fraction of the DOM pool in most lakes (Guillemette et al., 2016; Jones et al., 1998; Tranvik, 1992). As analytical methods are more likely to detect abundant compounds, we expected a higher number of metabolites of allochthonous origin. However, our result that Cluster 1, which regroups compounds primarily of autochthonous origin, contained more metabolites than Clusters 2 and 3 suggests a higher richness of DOM<sub>auto</sub> than of DOM<sub>allo</sub>. A possible explanation is that DOM<sub>auto</sub> contains more labile compounds and thus turns over faster and produces more compounds than more

slowly metabolized DOM<sub>allo</sub>. This idea is further supported by our observation that the sharp decline in the diversity of Cluster 1 after four weeks in the clear-water enclosures corresponds to decreasing chlorophyll-*a* concentrations. This suggests that a disruption of primary production, the putative key source process generating metabolites in Cluster 1, reduced metabolite diversity. A corollary of this conclusion is that properties of the DOM pool such as molecular diversity might be useful as indicators of particular metabolic processes such as primary production.

Heterotrophic bacteria in lakes barely assimilate the humic model substance used as source of cDOM in our study (HuminFeed<sup>®</sup>) (Lebret et al., 2018). This indicates that the dynamics of molecular diversity in Clusters 2 and 3, which putatively comprised metabolites from allochthonous sources, are primarily due to photodegradation. For instance, the prevalence in Cluster 3 of compounds with a high H:C ratio is indicative of photochemical degradation (Medeiros et al., 2015; Stubbins et al., 2010). Moreover, Shannon diversity increased at the beginning of our photodegradation experiment in Erlenmeyer flasks that precluded microbial activity, and decreased toward the end, suggesting that photodegradation of allochthonous compounds can indeed substantially alter molecular diversity.

#### 4.5. Application to Field Data

The humic substance used in our experiment is particularly resistant to microbial degradation, as are all alkaline extracts of humic substances (Kleber & Lehmann, 2019). Therefore, our enclosure experiment likely favored photodegradation over microbial transformations of the added allochthonous organic matter (Attermeyer et al., 2013). Therefore, we also used a published data set of 109 lakes in Sweden (Kellerman et al., 2015) and applied the same network analysis to assess whether similar patterns emerged as in the enclosure and photodegradation experiments. We reasoned that this approach captures a large portion of the processes transforming DOM in lakes, including processes triggered by brownification and nutrient enrichment. Consistent with this hypothesis, our analysis of the large set of field data produced the same metabolite clusters as the data from our enclosure experiment, which underpins the value of our approach. Similar to the results of the enclosure experiment, Cluster 1 of the field data set appeared to be of autochthonous origin, whereas the metabolites in Clusters 2 and 3 likely had an allochthonous origin. However, a notable difference was that more than 95% of the metabolites identified in the field data were associated with Clusters 1 and 2, so that Cluster 3 was much less prominent, possibly indicating major differences in the chemical nature of natural cDOM in lakes compared to the HuminFeed<sup>®</sup> used in our experiments.

## 5. Conclusion

In this study, we applied network analysis to identify source processes generating organic metabolites dissolved in lake water. The approach is based on an unconstrained data exploration instead of testing for effects based on significance thresholds (Wasserstein & Lazar, 2016). The network analysis produced a set of metabolite clusters which could be related to source processes and stressor impacts, and provided insights into the association between metabolites. Thus, we illustrate how ultrahigh-resolution mass spectrometry can partly resolve the molecular composition of thousands of metabolites in lake water and thus overcome the crude classification of DOM into allochthonous and autochthonous organic matter. Associating a given metabolite cluster with a particular stressor yet remains challenging, but such efforts could benefit from integrating additional information such as total phosphorus or DOC concentrations or results from PARAFAC modeling. Overall, our network analysis of metabolites suggests that the ecosystem metabolome, representing a vast suite of organic compounds potentially involved in numerous physical, chemical and biological transformation processes, is a useful concept for ecosystem-scale analyses. Its value could include the possibility of disentangling effects of multiple stressors such as browning and nutrient enrichment on lakes. Potentially, this opens opportunities to assess impacts of global change and other human activities on aquatic ecosystems, and to inform lake monitoring and management. Moreover, the concept could be extended to other ecosystems, particularly along flow paths of water and organic matter from streams and rivers to the oceans.

## Data Availability Statement

Data and computer code are available as supporting information. All responsibilities for the content of this publication are assumed by the authors. Data have been deposited on Pangea (<https://doi.pangaea.de/10.1594/PANGAEA.920886>).

## Acknowledgments

The authors are indebted to the LakeLab team involved in setting up and maintaining the experimental field facility and sampling. The authors also thank H. Osterholz and the technical staff at the ICBM, Oldenburg, for their help in FT-ICR-MS analyses. Funding was received through the projects MARS (Managing Aquatic ecosystems and water Resources under multiple Stress) of the EU Commission ([www.mars-project.eu](http://www.mars-project.eu); contract no. 603378), ILES (Illuminating Lake Ecosystems) as part of the Leibniz Competition (SAW-2015-IGB-1 415), and BIBS (Bridging in Biodiversity Science; funding no. 01LC1501G) supported by the German Federal Ministry of Education and Research (BMBF). An infrastructure grant by the BMBF (no. 033L041B) and a Core Facility grant by the German Research Foundation (DFG, no. GE 1775/2-1) enabled the construction and operation of the enclosure facility. Open access funding enabled and organized by Projekt DEAL.

## References

- Attermeyer, K., Premke, K., Hornick, T., Hilt, S., & Grossart, H. P. (2013). Ecosystem-level studies of terrestrial carbon reveal contrasting bacterial metabolism in different aquatic habitats. *Ecology*, *94*, 2754–2766. <https://doi.org/10.1890/13-0420.1>
- Attermeyer, K., Tittel, J., Allgaier, M., Frindte, K., Wurzbacher, C., Hilt, S., et al. (2015). Effects of light and autochthonous carbon additions on microbial turnover of allochthonous organic carbon and community composition. *Microbial Ecology*, *69*(2), 361–371. <https://doi.org/10.1007/s00248-014-0549-4>
- Bergström, A. K., & Karlsson, J. (2019). Light and nutrient control phytoplankton biomass responses to global change in northern lakes. *Global Change Biology*, *25*, 2021–2029. <https://doi.org/10.1111/gcb.14623>
- Bracchini, L., Dattilo, A. M., Hull, V., Loisselle, S. A., Nannicini, L., Picchi, M. P., et al. (2010). Spatial and seasonal changes in optical properties of autochthonous and allochthonous chromophoric dissolved organic matter in a stratified mountain lake. *Photochemical & Photobiological Sciences*, *9*, 304–314. <https://doi.org/10.1039/b9pp00129h>
- Brandão, L. P. M., Brighenti, L. S., Staehr, P. A., Asmala, E., Massicotte, P., Tonetta, D., et al. (2018). Distinctive effects of allochthonous and autochthonous organic matter on CDOM spectra in a tropical lake. *Biogeosciences*, *15*, 2931–2943. <https://doi.org/10.5194/bg-15-2931-2018>
- Brockman, S. A., Roden, E. V., & Hegeman, A. D. (2018). Van Krevelen diagram visualization of high resolution-mass spectrometry metabolomics data with OpenVanKrevelen. *Metabolomics*, *14*(4), 48. <https://doi.org/10.1007/s11306-018-1343-y>
- Brothers, S., Köhler, J., Attermeyer, K., Grossart, H. P., Mehner, T., Meyer, N., et al. (2014). A feedback loop links brownification and anoxia in a temperate, shallow lake. *Limnology and Oceanography*, *59*. <https://doi.org/10.4319/lo.2014.59.4.1388>
- Camacho, D., de la Fuente, A., & Mendes, P. (2005). The origin of correlations in metabolomics data. *Metabolomics*, *1*, 53–63. <https://doi.org/10.1007/s11306-005-1107-3>
- Christmann, D. R., Crouch, S. R., Holland, J. F., & Timmlck, A. (1980). Correction of right-angle molecular fluorescence measurements for absorption of fluorescence radiation. *Analytical Chemistry*, *52*, 291–295. <https://doi.org/10.1021/ac50052a019>
- Clauset, A., Newman, M. E. J., & Moore, C. (2004). Finding community structure in very large networks. *Physical Review E*, *70*, 066111. <https://doi.org/10.1103/PhysRevE.70.066111>
- Cory, R. M., & Kling, G. W. (2018). Interactions between sunlight and microorganisms influence dissolved organic matter degradation along the aquatic continuum. *Limnology and Oceanography Letters*, *3*, 102–116. <https://doi.org/10.1002/lo.10060>
- Creed, I. F., McKnight, D. M., Pellerin, B. A., Green, M. B., Bergamaschi, B. A., Aiken, G. R., et al. (2015). The river as a chemostat: Fresh perspectives on dissolved organic matter flowing down the river continuum. *Canadian Journal of Fisheries and Aquatic Sciences*, *72*, 1272–1285. <https://doi.org/10.1139/cjfas-2014-0400>
- Danczak, R. E., Chu, R. K., Fansler, S. J., Goldman, A. E., Graham, E. B., Tfaily, M. M., et al. (2020). Using metacommunity ecology to understand environmental metabolomes. *Nature Communications*, *11*, 6369. <https://doi.org/10.1038/s41467-020-19989-y>
- D'Andrilli, J., Cooper, W. T., Foreman, C. M., & Marshall, A. G. (2015). An ultrahigh-resolution mass spectrometry index to estimate natural organic matter lability. *Rapid Communications in Mass Spectrometry*, *29*, 2385–2401. <https://doi.org/10.1002/rcm.7400>
- Davies, P. T., & Tso, M. K.-S. (1982). Procedures for reduced-rank regression. *Applied Statistics*, *31*(3), 244–255. <https://doi.org/10.2307/2347998>
- del Campo, R., Gómez, R., & Singer, G. (2019). Dry phase conditions prime wet-phase dissolved organic matter dynamics in intermittent rivers. *Limnology and Oceanography*, *64*, 1966–1979. <https://doi.org/10.1002/lno.11163>
- Dittmar, T., Koch, B., Hertkorn, N., & Kattner, G. (2008). A simple and efficient method for the solid-phase extraction of dissolved organic matter (SPE-DOM) from seawater. *Limnology and Oceanography: Methods*, *6*, 230–235. <https://doi.org/10.4319/lom.2008.6.230>
- Dittmar, T., Whitehead, K., Minor, E. C., & Koch, B. P. (2007). Tracing terrigenous dissolved organic matter and its photochemical decay in the ocean by using liquid chromatography/mass spectrometry. *Marine Chemistry*, *107*, 378–387. <https://doi.org/10.1016/j.marchem.2007.04.006>
- Doncheva, N. T., Assenov, Y., Domingues, F. S., & Albrecht, M. (2012). Topological analysis and interactive visualization of biological networks and protein structures. *Nature Protocols*, *7*, 670–685. <https://doi.org/10.1038/nprot.2012.004>
- Evans, C. D., Monteith, D. T., & Cooper, D. M. (2005). Long-term increases in surface water dissolved organic carbon: Observations, possible causes and environmental impacts. *Environmental Pollution*, *137*, 55–71. <https://doi.org/10.1016/j.envpol.2004.12.031>
- Fasching, C., Behounek, B., Singer, G. A., & Battin, T. J. (2014). Microbial degradation of terrigenous dissolved organic matter and potential consequences for carbon cycling in brown-water streams. *Scientific Reports*, *4*, 4981. <https://doi.org/10.1038/srep04981>
- Finstad, A. G., Helland, I. P., Ugedal, O., Hesthagen, T., & Hessen, D. O. (2014). Unimodal response of fish yield to dissolved organic carbon. *Ecology Letters*, *17*, 36–43. <https://doi.org/10.1111/ele.12201>
- Gautam, C. R., & Yadav, A. K. (2013). Synthesis and optical investigations on (Ba, Sr)TiO<sub>3</sub> borosilicate glasses doped with La<sub>2</sub>O<sub>3</sub>. *Optics and Photonics Journal*, *3*, 1–7. <https://doi.org/10.4236/opj.2013.34A001>
- Giling, D. P., Nejtgaard, J. C., Berger, S. A., Grossart, H. P., Kirillin, G., Penske, A., et al. (2017). Thermocline deepening boosts ecosystem metabolism: Evidence from a large-scale lake enclosure experiment simulating a summer storm. *Global Change Biology*, *23*, 1448–1462. <https://doi.org/10.1111/gcb.13512>
- Guillemette, F., McCallister, S. L., & del Giorgio, P. A. (2016). Selective consumption and metabolic allocation of terrestrial and algal carbon determine allochthony in lake bacteria. *The ISME Journal*, *10*, 1373–1382. <https://doi.org/10.1038/ismej.2015.215>
- Haaber, J., & Middelboe, M. (2009). Viral lysis of *Phaeocystis pouchetii*: Implications for algal population dynamics and heterotrophic C, N and P cycling. *The ISME Journal*, *3*, 430–441. <https://doi.org/10.1038/ismej.2008.125>
- Hastie, T. (2015). Package 'gam.' R Package Version. [https://doi.org/10.1016/0169-5347\(88\)90124-3](https://doi.org/10.1016/0169-5347(88)90124-3)
- Hastie, T. J., & Tibshirani, R. J. (1990). *Generalized Additive Models*. Monographs on Statistics and Applied Probability, 43, Chapman & Hall. <https://doi.org/10.1016/j.csda.2010.05.004>



- Hering, D., Carvalho, L., Argillier, C., Beklioglu, M., Borja, A., Cardoso, A. C., et al. (2015). Managing aquatic ecosystems and water resources under multiple stress: An introduction to the MARS project. *The Science of the Total Environment*, 503–504, 10–21. <https://doi.org/10.1016/j.scitotenv.2014.06.106>
- Herzprung, P., Osterloh, K., von Tümpling, W., Harir, M., Hertkorn, N., Schmitt-Kopplin, P., et al. (2017). Differences in DOM of rewetted and natural peatlands—Results from high-field FT-ICR-MS and bulk optical parameters. *The Science of the Total Environment*, 586, 770–781. <https://doi.org/10.1016/j.scitotenv.2017.02.054>
- Herzprung, P., Von Tümpling, W., Hertkorn, N., Harir, M., Büttner, O., Bravidor, J., et al. (2012). Variations of DOM quality in inflows of a drinking water reservoir: Linking of van Krevelen diagrams with EEMF spectra by rank correlation. *Environmental Science & Technology*, 46, 5511–5518. <https://doi.org/10.1021/es300345c>
- Hothorn, A. T., Zeileis, A., Millo, G., & Mitchell, D. (2011). Package 'lme4'. *R News*.
- IPCC. (2014). Climate Change 2014: Synthesis report. *Contribution of Working Groups I, II and III to the Fifth Assessment Report of the Intergovernmental Panel on Climate Change*. Cambridge, UK: Cambridge University Press.
- Jeong, H., Tombor, B., Albert, R., Oltval, Z. N., & Barabási, A. L. (2000). The large-scale organization of metabolic networks. *Nature*, 407, 651–654. <https://doi.org/10.1038/35036627>
- Jones, R. I., Grey, J., Sleep, D., & Quarmby, C. (1998). An assessment, using stable isotopes, of the importance of allochthonous organic carbon sources to the pelagic food web in Loch Ness. *Proceedings of the Royal Society B*, 265, 105–110. <https://doi.org/10.1098/rspb.1998.0270>
- Karlsson, J., Byström, P., Ask, J., Ask, P., Persson, L., & Jansson, M. (2009). Light limitation of nutrient-poor lake ecosystems. *Nature*, 460, 506–509. <https://doi.org/10.1038/nature08179>
- Kellerman, A. M. (2015). *Molecular dissolved organic matter composition in lakes across Sweden as PARAFAC components and optical indices*. PANGAEA. <https://doi.org/10.1594/PANGAEA.844883>
- Kellerman, A. M., Dittmar, T., Kothawala, D. N., & Tranvik, L. J. (2014). Chemodiversity of dissolved organic matter in lakes driven by climate and hydrology. *Nature Communications*, 5, 3804. <https://doi.org/10.1038/ncomms4804>
- Kellerman, A. M., Kothawala, D. N., Dittmar, T., & Tranvik, L. J. (2015). Persistence of dissolved organic matter in lakes related to its molecular characteristics. *Nature Geoscience*, 8, 454–457. <https://doi.org/10.1038/NGEO2440>
- Kleber, M., & Lehmann, J. (2019). Humic substances extracted by alkali are invalid proxies for the dynamics and functions of organic matter in terrestrial and aquatic ecosystems. *Journal of Environmental Quality*, 48, 207–216. <https://doi.org/10.2134/jeq2019.01.0036>
- Koch, B. P., & Dittmar, T. (2006). From mass to structure: An aromaticity index for high-resolution mass data of natural organic matter. *Rapid Communications in Mass Spectrometry*, 20, 926–932. <https://doi.org/10.1002/rcm.2386>
- Köhler, S. J., Kothawala, D., Futter, M. N., Liungman, O., & Tranvik, L. (2013). In-lake processes offset increased terrestrial inputs of dissolved organic carbon and color to lakes. *PloS One*, 8, e70598. <https://doi.org/10.1371/journal.pone.0070598>
- Kreyling, J., Schweiger, A. H., Bahn, M., Ineson, P., Migliavacca, M., Morel-Journel, T., et al. (2018). To replicate, or not to replicate – that is the question: how to tackle nonlinear responses in ecological experiments. *Ecology Letters*, 21, 1629–1638. <https://doi.org/10.1111/ele.13134>
- Kritzberg, E. S., Hasselquist, E. M., Škerlep, M., Löfgren, S., Olsson, O., Stadmark, J., et al. (2020). Browning of freshwaters: Consequences to ecosystem services, underlying drivers, and potential mitigation measures. *Ambio*, 49, 375–390. <https://doi.org/10.1007/s13280-019-01227-5>
- Kurtz, Z. D., Müller, C. L., Miraldi, E. R., Littman, D. R., Blaser, M. J., & Bonneau, R. A. (2015). Sparse and compositionally robust inference of microbial ecological networks. *PLoS Computational Biology*, 11, e1004226. <https://doi.org/10.1371/journal.pcbi.1004226>
- Larsson, U., & Hagström, Å. (1982). Fractionated phytoplankton primary production, exudate release and bacterial production in a Baltic eutrophication gradient. *Marine Biology*, 67, 57–70. <https://doi.org/10.1007/BF00397095>
- Lebret, K., Langenheder, S., Colinas, N., Östman, Ö., & Lindström, E. S. (2018). Increased water colour affects freshwater plankton communities in a mesocosm study. *Aquatic Microbial Ecology*, 81, 1–17. <https://doi.org/10.3354/ame01858>
- Leech, D. M., Pollard, A. I., Labou, S. G., & Hampton, S. E. (2018). Fewer blue lakes and more murky lakes across the continental US: Implications for planktonic food webs. *Limnology and Oceanography*, 63, 2661–2680. <https://doi.org/10.1002/lno.10967>
- Lesaulnier, C. C., Herbold, C. W., Pelikan, C., Berry, D., Gérard, C., Le Coz, X., et al. (2017). Bottled aqua incognita: microbiota assembly and dissolved organic matter diversity in natural mineral waters. *Microbiome*, 5, 126. <https://doi.org/10.1186/s40168-017-0344-9>
- Lewis, W. M., & Wurtsbaugh, W. A. (2008). Control of lacustrine phytoplankton by nutrients: Erosion of the phosphorus paradigm. *International Review of Hydrobiology*, 93, 446–465. <https://doi.org/10.1002/iroh.200811065>
- Lusk, M. G., & Toor, G. S. (2016a). Biodegradability and molecular composition of dissolved organic nitrogen in urban stormwater runoff and outflow water from a stormwater retention pond. *Environmental Science & Technology*, 50, 3391–3398. <https://doi.org/10.1021/acs.est.5b05714>
- Lusk, M. G., & Toor, G. S. (2016b). Dissolved organic nitrogen in urban streams: Biodegradability and molecular composition studies. *Water Research*, 96, 225–235. <https://doi.org/10.1016/j.watres.2016.03.060>
- Maizel, A. C., Li, J., & Remucal, C. K. (2017). Relationships between dissolved organic matter composition and photochemistry in lakes of diverse trophic status. *Environmental Science & Technology*, 51, 9624–9632. <https://doi.org/10.1021/acs.est.7b01270>
- María, M.-P., Nieto-cid, M., Osterholz, H., Catala, T., Reche, I., Dittmar, T., et al. (2017). Molecular composition of dissolved organic matter in the Mediterranean Sea. *Limnology and Oceanography*, 62, 2699–2712. <https://doi.org/10.1038/s41598-017-03735-4>
- Medeiros, P. M., Seidel, M., Ward, N. D., Carpenter, E. J., Gomes, H. R., Niggemann, J., et al. (2015). Fate of the Amazon River dissolved organic matter in the tropical Atlantic Ocean. *Global Biogeochemical Cycles*, 29, 677–690. <https://doi.org/10.1002/2015GB005115>
- Mentges, A., Feenders, C., Seibt, M., Blasius, B., & Dittmar, T. (2017). Functional molecular diversity of marine dissolved organic matter is reduced during degradation. *Frontiers in Marine Science*, 4, 194. <https://doi.org/10.3389/fmars.2017.00194>
- Mínguez, L., Sperfeld, E., Berger, S. A., Nejstgaard, J. C., & Gessner, M. O. (2019). Changes in food characteristics reveal indirect effects of lake browning on zooplankton performance. *Limnology and Oceanography*, 65, 1028–1040. <https://doi.org/10.1002/lno.11367>
- Murphy, K. R., Stedmon, C. A., Graeber, D., & Bro, R. (2013). Fluorescence spectroscopy and multi-way techniques PARAFAC. *Analytical Methods*, 5, 6557–6566. <https://doi.org/10.1039/c3ay41160e>
- Murphy, K. R., Stedmon, C. A., Waite, T. D., & Ruiz, G. M. (2008). Distinguishing between terrestrial and autochthonous organic matter sources in marine environments using fluorescence spectroscopy. *Marine Chemistry*, 108, 40–58. <https://doi.org/10.1016/j.marchem.2007.10.003>
- Muscarella, M. E., Boot, C. M., Broeckling, C. D., & Lennon, J. T. (2019). Resource heterogeneity structures aquatic bacterial communities. *The ISME Journal*, 13, 2183–2195. <https://doi.org/10.1038/s41396-019-0427-7>

- Nejstgaard, J. C., Frischer, M. E., Verity, P. G., Anderson, J. T., Jacobsen, A., Zirbel, M. J., et al. (2006). Plankton development and trophic transfer in seawater enclosures with nutrients and *Phaeocystis pouchetii* added. *Marine Ecology Progress Series*, 321, 99–121. <https://doi.org/10.3354/meps321099>
- Noble, R. T., & Fuhrman, J. A. (1999). Breakdown and microbial uptake of marine viruses and other lysis products. *Aquatic Microbial Ecology*, 20, 1–11. <https://doi.org/10.3354/ame020001>
- Oksanen, J., Blanchet, F. G., Kindt, R., Legendre, P., Minchin, P. R., O'Hara, R. B., et al. (2013). Package 'vegan.' *R Package Version 2.5–2*. <https://doi.org/10.4135/9781412971874.n145>
- Osburn, C. L., & Stedmon, C. A. (2011). Linking the chemical and optical properties of dissolved organic matter in the Baltic-North Sea transition zone to differentiate three allochthonous inputs. *Marine Chemistry*, 126, 281–294. <https://doi.org/10.1016/j.marchem.2011.06.007>
- Pace, M. L., Cole, J. J., Carpenter, S. R., Kitchell, J. F., Hodgson, J. R., Van De Bogert, M. C., et al. (2004). Whole-lake carbon-13 additions reveal terrestrial support of aquatic food webs. *Nature*, 427, 240–243. <https://doi.org/10.1038/nature02227>
- Pereira, R., Isabella Bovolo, C., Spencer, R. G. M., Hernes, P. J., Tipping, E., Vieth-Hillebrand, A., et al. (2014). Mobilization of optically invisible dissolved organic matter in response to rainstorm events in a tropical forest headwater river. *Geophysical Research Letters*, 41, 1202–1208. <https://doi.org/10.1002/2013GL058658>
- Pesenson, M. Z., Suram, S. K., & Gregoire, J. M. (2015). Statistical analysis and interpolation of compositional data in materials science. *ACS Combinatorial Science*, 17, 130–136. <https://doi.org/10.1021/co5001458>
- Phong, D. D., & Hur, J. (2015). Insight into photocatalytic degradation of dissolved organic matter in UVA/TiO<sub>2</sub> systems revealed by fluorescence EEM-PARAFAC. *Water Research*, 87, 119–126. <https://doi.org/10.1016/j.watres.2015.09.019>
- R Core team. (2017). *R: A language and environment for statistical computing*. R Foundation for Statistical Computing. <http://www.R-Project.Org/>. <https://doi.org/10.2788/95827>
- Riedel, T., Zark, M., Vähätalo, A. V., Niggemann, J., Spencer, R. G. M., Hernes, P. J., & Dittmar, T. (2016). Molecular signatures of biogeochemical transformations in dissolved organic matter from ten world rivers. *Frontiers of Earth Science*, 4, 85. <https://doi.org/10.3389/feart.2016.00085>
- Ripley, B., Venables, B., Bates, D. M., Hornik, K., Gebhardt, A., & Firth, D. (2019). Package 'MASS' (Version 7.3–51.4). Cran-R Project
- Roulet, N., & Moore, T. R. (2006). Browning the waters. *Nature*, 444, 283–284. <https://doi.org/10.1038/444283a>
- Šantl-Temkiv, T., Finster, K., Dittmar, T., Hansen, B. M., Thyraug, R., et al. (2013). Hailstones: A window into the microbial and chemical inventory of a storm cloud. *PLoS One*, 8, e53550. <https://doi.org/10.1371/journal.pone.0053550>
- Schindler, D. W., Carpenter, S. R., Chapra, S. C., Hecky, R. E., & Orihel, D. M. (2016). Reducing phosphorus to curb lake eutrophication is a success. *Environmental Science & Technology*, 50, 8923–8929. <https://doi.org/10.1021/acs.est.6b02204>
- Shannon, C. E. C., & Weaver, W. (1949). *The mathematical theory of information*. Urbana University of Illinois Press. <https://doi.org/10.1007/978-1-4615-0975-2>
- Singer, G. A., Fasching, C., Wilhelm, L., Niggemann, J., Steier, P., Dittmar, T., & Battin, T. J. (2012). Biogeochemically diverse organic matter in Alpine glaciers and its downstream fate. *Nature Geoscience*, 5, 710–714. <https://doi.org/10.1038/ngeo1581>
- Smith, V. H., Tilman, G. D., & Nekola, J. C. (1999). Eutrophication: Impacts of excess nutrient inputs on freshwater, marine, and terrestrial ecosystems. *Environmental Pollution*, 100, 179–196. [https://doi.org/10.1016/S0269-7491\(99\)00091-3](https://doi.org/10.1016/S0269-7491(99)00091-3)
- Solomon, C. T., Jones, S. E., Weidel, B. C., Buffam, I., Fork, M. L., Karlsson, J., et al. (2015). Ecosystem consequences of changing inputs of terrestrial dissolved organic matter to lakes: Current knowledge and future challenges. *Ecosystems*, 18(3), 376–389. <https://doi.org/10.1007/s10021-015-9848-y>
- Spencer, R. G. M., Stubbins, A., Hernes, P. J., Baker, A., Mopper, K., Aufdenkampe, A. K., et al. (2009). Photochemical degradation of dissolved organic matter and dissolved lignin phenols from the Congo River. *Journal of Geophysical Research*, 114, G03010. <https://doi.org/10.1029/2009JG000968>
- Spirin, V., Gelfand, M. S., Mironov, A. A., & Mirny, L. A. (2006). A metabolic network in the evolutionary context: Multiscale structure and modularity. *Proceedings of the National Academy of Sciences of the United States of America*, 103, 8774–8779. <https://doi.org/10.1073/pnas.0510258103>
- Stedmon, C. A., & Markager, S. (2005). Tracing the production and degradation of autochthonous fractions of dissolved organic matter by fluorescence analysis. *Limnology and Oceanography*, 50, 1415–1426. <https://doi.org/10.4319/lo.2005.50.5.1415>
- Stedmon, C. A., Thomas, D. N., Granskog, M., Kaartokallio, H., Papadimitriou, S., & Kuosa, H. (2007). Characteristics of dissolved organic matter in baltic coastal sea ice: Allochthonous or autochthonous origins? *Environmental Science & Technology*, 41, 7273–7279. <https://doi.org/10.1021/es071210f>
- Strock, K. E., Theodore, N., Gawley, W. G., Ellsworth, A. C., & Saros, J. E. (2017). Increasing dissolved organic carbon concentrations in northern boreal lakes: Implications for lake water transparency and thermal structure. *Journal of Geophysical Research: Biogeosciences*, 122, 1022–1035. <https://doi.org/10.1002/2017JG003767>
- Stubbins, A., Spencer, R. G. M., Chen, H., Hatcher, P. G., Mopper, K., Hernes, P. J., et al. (2010). Illuminated darkness: Molecular signatures of Congo River dissolved organic matter and its photochemical alteration as revealed by ultrahigh precision mass spectrometry. *Limnology and Oceanography*, 55, 1467–1477. <https://doi.org/10.4319/lo.2010.55.4.1467>
- Su, G., Kuchinsky, A., Morris, J. H., States, D. J., & Meng, F. (2010). Glay: Community structure analysis of biological networks. *Bioinformatics*, 26, 3135–3137. <https://doi.org/10.1093/bioinformatics/btq596>
- Sugimoto, M., Wong, D. T., Hirayama, A., Soga, T., & Tomita, M. (2010). Capillary electrophoresis mass spectrometry-based saliva metabolomics identified oral, breast and pancreatic cancer-specific profiles. *Metabolomics*, 6, 78–95. <https://doi.org/10.1007/s11306-009-0178-y>
- Tansley, A. G. (1939). British ecology during the past quarter-century: The plant community and the ecosystem. *Journal of Ecology*, 27, 513–530. <https://doi.org/10.2307/2256377>
- Tranvik, L. J. (1992). Allochthonous dissolved organic matter as an energy source for pelagic bacteria and the concept of the microbial loop. *Hydrobiologia*, 229, 107–114. <https://doi.org/10.1007/BF00006994>
- Velthuis, M., De Senerpont Domis, L. N., Frenken, T., Stephan, S., Kazanjian, G., Aben, R., et al. (2017). Warming advances top-down control and reduces producer biomass in a freshwater plankton community. *Ecosphere*, 8, e01651. <https://doi.org/10.1002/ecs2.1651>
- Von Einem, J., & Granéli, W. (2010). Effects of fetch and dissolved organic carbon on epilimnion depth and light climate in small forest lakes in southern Sweden. *Limnology and Oceanography*, 55, 920–930. <https://doi.org/10.4319/lo.2009.55.2.0920>
- Wasserstein, R. L., & Lazar, N. A. (2016). The ASA's statement on p-values: Context, process, and purpose. *The American Statistician*, 70, 129–133. <https://doi.org/10.1080/00031305.2016.1154108>
- Zherebker, A. Y., Perminova, I. V., Konstantinov, A. I., Volikov, A. B., Kostyukevich, Y. I., Kononikhin, A. S., & Nikolaev, E. N. (2016). Extraction of humic substances from fresh waters on solid-phase cartridges and their study by Fourier transform ion cyclotron resonance mass spectrometry. *Journal of Analytical Chemistry*, 71, 372–378. <https://doi.org/10.1134/S1061934816040109>

Zhou, Y., Davidson, T. A., Yao, X., Zhang, Y., Jeppesen, E., de Souza, J. G., et al. (2018). How autochthonous dissolved organic matter responds to eutrophication and climate warming: Evidence from a cross-continental data analysis and experiments. *Earth-Science Reviews*, 185, 928–937. <https://doi.org/10.1016/j.earscirev.2018.08.013>